J Musculoskelet Neuronal Interact 2019; 19(1):13-20

Journal of Musculoskeletal and Neuronal Interactions JMNI

Original Article

Mechanobiological analysis of porcine spines instrumented with intra-vertebral staples

Alejandra Mejia Jaramillo[1,2], Carl-Éric Aubin[1,2,3], Bahe Hachem[1,2], Irene Londono[2], Juliette Pelletier[1], Stefan Parent[2,3], Isabelle Villemure[1,2]

[1]Polytechnique Montréal, Canada; [2]Sainte-Justine University Hospital Center, Canada; [3]Univerisity of Montreal, Canada

Abstract

Objective: To characterize growth plate histology of porcine spines instrumented with a new intra-vertebral staple. **Methods:** Spinal segments (T7-T9) previously instrumented with an intra-vertebral staple (experimental group, n=7) or non-instrumented (control group, n=4) underwent average growth rate (AGR), and histomorphometric measurements: heights of proliferative (PZH) and hypertrophic (HZH) growth plate zones, hypertrophic cells height (CH), and the number of proliferative chondrocytes per column (CC). These measurements were done over three regions: (1) left side; (2) middle; (3) right side (instrumented side). The two groups were analyzed by comparing the difference between results for regions 1 and 3 (Dif-R1R3). **Results:** A significantly higher Dif-R1R3 was found for AGR and HZH for the experimental group as compared with controls. This Dif-R1R3 was also significantly higher for CC at T8 level, CH at T7 level and PZH at both levels. No significant changes for the Dif-R1R3 were observed in the adjacent vertebrae (T11-T12). **Conclusions:** This study confirmed the local growth modulation capacity of the intra-vertebral staple, translated at the histomorphometric level by a significant reduction in all parameters, but not in all spinal levels. Further analyses are needed to confirm the regional effect, especially for the intervertebral disc and other connective tissues.

Keywords: Growth Modulation, Fusionless Implant, Scoliosis, Hypertrophic Zone, Proliferative Zone

Introduction

Adolescent Idiopathic Scoliosis (AIS) is a 3D spinal deformity, presenting curvature(s) in the coronal plane but also vertebral rotation in the transverse plane and an altered sagittal profile. Curve progression might be related to factors such as the remaining bone growth, the degree of the initial curvature[1,2], and some of its morphological parameters like sagittal intervertebral rotation, 3D wedging of the apical disks, vertebral axial rotation, among others[3]. Based on the estimation of curve progression, a proper treatment should be chosen. Generally, a patient with a curvature of more than 45° and limited remaining growth will undergo spinal instrumentation and fusion, a highly invasive surgery associated with important risks and mobility impacts in these young patients[4-6]. For pediatric scoliotic patients presenting a moderate spinal deformity with significant growth remaining, compressive fusionless approaches can be considered (off label procedure) to correct the curvatures, hence avoiding spinal arthrodesis. Compressive fusionless techniques aim at progressively correcting the deformation using the remaining bone growth potential while preserving patients' mobility[7]. They are based on Hueter-Volkmann principle to reduce or increase vertebral growth by means of an increased pressure on the convex side of the curve, or a decreased pressure on concave side of the curve, respectively.

Longitudinal spine growth takes place in vertebral body epiphyseal growth plates by synthesizing cartilaginous tissue, which is further transformed into bone by endochondral ossification[8]. The growth plate is a connective tissue divided into three zones. The reserve zone includes chondrocytes in a relatively quiescent state. It supplies the proliferative

The authors have no conflict of interest.

Corresponding author: Isabelle Villemure, PhD Full Professor, Department of Mechanical Engineering, Polytechnique Montréal, C.P. 6079, Downtown Office, Montreal, Quebec, CANADA H3C 3A7
E-mail: isabelle.villemure@polymtl.ca

Edited by: G. Lyritis
Accepted 2 July 2018

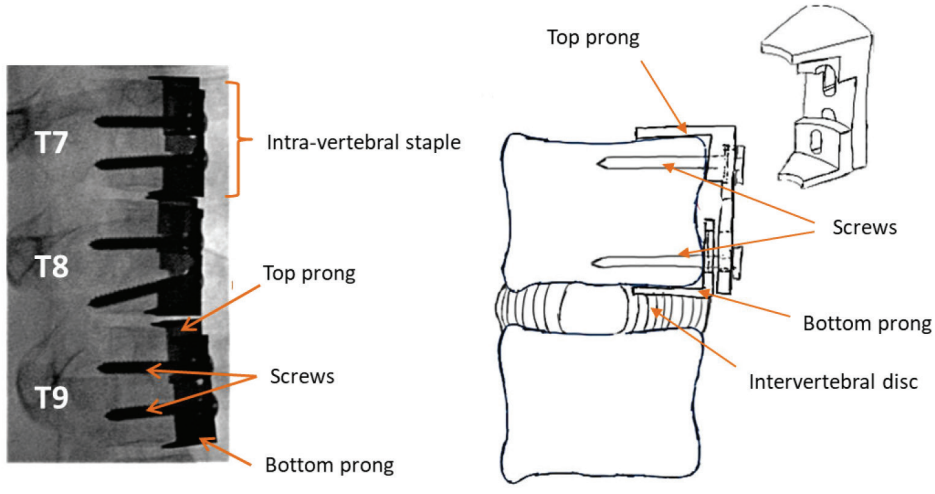

Figure 1. Intra-vertebral staple with 0.5 mm thick dual prongs with an approximate penetration of 5 mm. Intraoperative fluoroscopic image of implants insertion site (Image modified from[30]). GP: growth plate.

zone, where chondrocytes undergo division. Chondrocytes finally are pushed towards the hypertrophic zone, where they increase in volume and undergo apoptosis at the osteochondral junction. The growth process is based on the progression, as well as on changes of chondrocytes and their surrounding extracellular matrix composition through these three zones.

Fusionless compressive devices spanning a scoliotic curve segment, such as anterior vertebral body tethering and vertebral staples, have shown to progressively correct scoliotic curvatures with vertebral growth[9-13]. At the histological level, vertebral growth modulation was associated with decreased hypertrophic zone height and hypertrophic cells heights on the implant's side, as reported by experimental studies on pig models[14-16]. These changes occur in response to compressive stresses transmitted to the growth plates by the implant.

To avoid spanning the intervertebral disc (IVD), which is thought to lead to IVD degeneration[17], a new implant for the treatment of pediatric scoliosis was developed[18]. This implant, consisting of a staple, was designed to be fixed on the lateral side of the vertebral body, with its very thin prong affixed onto the superior growth plate of a given vertebra, below the contiguous annulus fibrosus, therefore without spanning of the IVD[18]. It has been tested, firstly in a rat tail model[19] and secondly in a porcine model[20]. The implant demonstrated its capability to reduce vertebral growth on the implant side and, when correctly placed, to preserve IVD health. A revised version of this implant allows the simultaneous action of two thin prongs on the superior and inferior vertebral growth plates of the same vertebra (Figure 1). This new intra-vertebral staple was tested in a pig model[21]. Its regional effects on the spine as well as on vertebral and intervertebral disc wedging were experimentally characterized[18]. However, its local effects have not yet been evaluated. Thus, the aim of this study was to comprehensively characterize the histology of the growth plates of porcine spinal segments instrumented with this double-sided intra-vertebral staple implant.

Materials and methods

Tissue collection

Spinal segments from eleven immature female pigs (Landrace/Yorkshire of 25-35 Kg; eleven weeks old) were used in this study, in continuity with the previous study[21]. In summary, seven animals (experimental group) underwent scoliosis induction using the new dual side prongs intra-vertebral staple presented above and four uninstrumented cases were used as controls (control group). During this previous study, the experimental animals were pre-operatively sedated. The surgery was performed in the left decubitus position in a sterile environment. The access to the tested segment (T7-T8-T9) was achieved via a right side thoracotomy between the seventh and eighth ribs. Both stainless steel (316L, UNS S31603) prongs of this new intra-vertebral staple were 0.5 mm thick, and were inserted between the IVD and the thin secondary ossification site just above the growth plate with an approximate penetration of 5 mm. After insertion, prongs were fixed using bone screws of 25x2.8 mm diameter (Figure 1). Site closure was performed after device insertion, and animals had a postoperative follow-up of 82 ± 2 days. A bicarbonate solution of Calcein (SigmaAldrich, Oakville, ON, Canada) was injected seven and one days prior to sacrifice at a dose of 15 mg/kg body weight, since during these days the intra-vertebral staple action over growth rate will be more highlighted, animals present a linear-like growth all along the follow-up, and Calcein will be

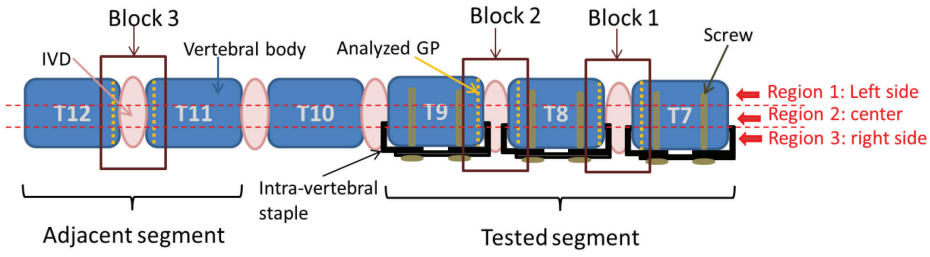

Figure 2. Vertebra-disc-vertebra blocks collected for both tested (blocks 1 and 2) and adjacent (block 3) segments of the porcine thoracic spine (coronal plane view). In each block, the corresponding analyzed GPs and its respective regions (left, center and right side) are shown. IVD: intervertebral disc, GP: growth plate.

kept from being released through osteoclasts activity before microscope observation. Animals were then euthanized by induction of deep anaesthesia followed by a lethal injection of saturated potassium chloride.

Immediately following euthanasia, thoracic spinal segments were collected for the present study. Three vertebra-disc-vertebra blocks (Figure 2) were dissected for each control or experimental animal and further fixed in 10% buffered formalin, dehydrated in increasing graded ethanol solutions and clarified in xylene before embedding in methylmetacrylate (MMA, Fisher Scientific, Ottawa, ON, Canada). Each block was first trimmed using a saw, equipped with a diamond knife (Buehler IsoMet 1000), and then cut along the longitudinal axis into ten series of six slices (6 µm) each, using a microtome (Leica SM2500).

Histological analyses

The evaluated growth plates are shown in Figure 2. Four spatially separated slices (30 µm), from each of the three blocks, were used for growth rate measurements, and four other spatially separated slices were used for histomorphometry measurements. All growth plates slices were virtually divided in three regions to better understand the local effects of the implant. Region 1 corresponded to the left (opposite side of the instrumentation for the experimental group), region 2 to the center and region 3 to the right (instrumented for the experimental group) spine side (Figure 2).

Histological staining and mounting

All slices were first deplasticized in two 30 min serial washes of EGMA (ethylene glycol methacrylate, Fisher Scientific), dried for 30 min, and then underwent one of the following protocols. For growth plate histomorphometry, slices were rehydrated in distilled water and stained with 1% Toluidine blue (Fisher Scientific) for 5 min, and washed with a citrate buffer solution. Following staining, slices were dehydrated in graded alcohols, followed by xylene and mounted with Permount mounting medium (Fisher Scientific). For growth rate measurements, slices were only deplasticized, transferred to graded ethanol solutions and xylene, and mounted with Permount.

Growth plate analyses

Three images were obtained, one per region of the analyzed growth plates, using an optical microscope (Leica DMR equipped with a Qimaging Retiga Camera). Growth rate and histomorphometric parameters were then evaluated on a total of 12 images (i.e. three images for each of the four evaluated slices) for each analyzed growth plate. All measurements were done using a custom-made Matlab application (R2014a, MathWorks, Natick, MA, USA)[22].

The average growth rate was evaluated on 10X-magnified images using Calcein labeling in the growth plate epiphyseal junction. The growth rate was evaluated as the distance between the two labels of Calcein further divided by the number of days (6) between the two injections (Figure 3a). The average growth rate was estimated as the mean of 35 to 45 height measurements taken parallel to the longitudinal growth direction and evenly separated in each of the 12 images[23].

Four histomorphometric parameters were analyzed on the vertebral growth plate stained with Toluidine blue observed under the microscope with a magnification of 20X. The hypertrophic and proliferative zone heights were evaluated similarly to average growth rate (Figure 3b). A total of 50 to 70 heights parallel to the longitudinal growth direction were evaluated and averaged on each of the 12 images for the hypertrophic and proliferative zones. Hypertrophic cells height was measured as the mean distance between the upper and the lower limit of a total of 120 hypertrophied chondrocytes, which means 10 randomly chosen cells per image (Figure 3c). Finally, regarding the number of chondrocytes per column, the analysis consisted of counting, in a total of 60 randomly chosen columns of proliferative chondrocytes, the number of cells per 100 µm (Figure 3d).

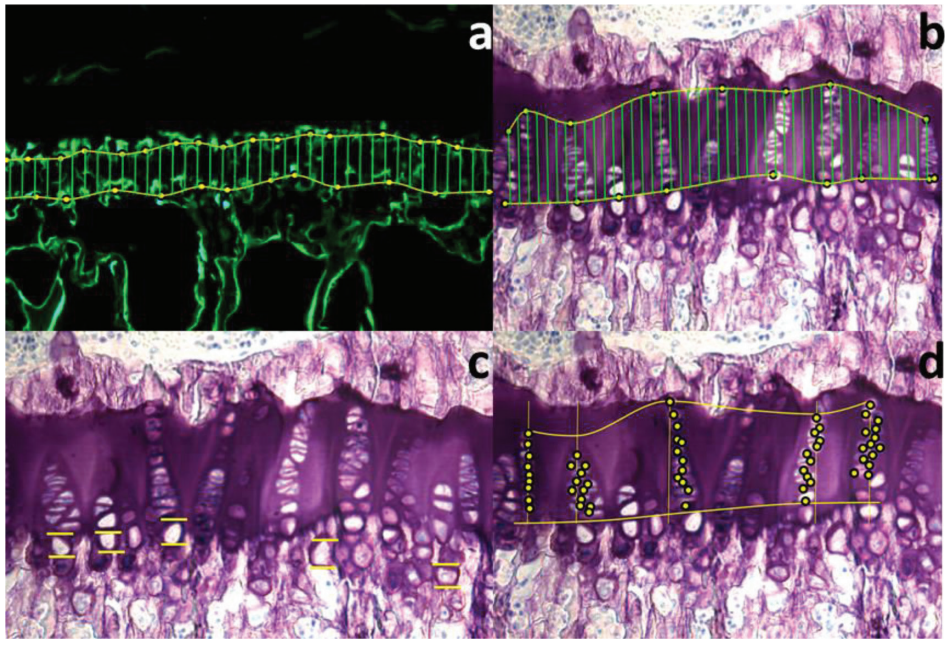

Figure 3. Growth plate section embedded in plastic and prepared with (a) Calcein labeling for growth rate measurement; or stained with Toluidine blue for (b) hypertrophic and proliferative zone height measurement, (c) hypertrophic cells height and (d) the number of chondrocytes per column.

Table 1. Growth plate parameters (three regions combined) for tested and adjacent segments of control and experimental groups (mean value ± SEM). AGR: average growth rate. HZH: hypertrophic zone height. PZH: proliferative zone height. CH: hypertrophic cells height. CC: number of proliferative chondrocytes per column.

	Tested segments (T7-T8-T9)		Adjacent segments (T11-T12)	
Parameter	**Control (n=4)**	**Experimental (n=7)**	**Control (n=4)**	**Experimental (n=7)**
AGR (μm/day)	10.1 ± 0.8	8.6 ± 0.6	10.6 ± 0.5	9.7 ± 0.6
HZH (μm)	55.9 ± 1.8	51.5 ± 2.2	48.8 ± 1.5	49.3 ± 1.9
PZH (μm)	63.2 ± 2.3	65.3 ± 2.3	68.5 ± 1.9	66.3 ± 1.2
CH (μm)	18.1 ± 0.6	17.7 ± 0.5	15.8 ± 0.5	15.5 ± 0.4
CC (cells /100 μm)	13.0 ± 0.8	13.4 ± 0.5	13.8 ± 0.4	13.9 ± 0.3

Statistical analyses

Statistical analyses were performed using STATISTICA 13.3 software package (Statistica, StatSoft Inc., Tulsa, Oklahoma, USA). First, all data was screened with a Shapiro Wilk W test to verify normality. Then, a one-way ANOVA for repeated measures was used to detect differences between the means obtained in each group (control and experimental) when subtracting results obtained for region 3 from those obtained for region 1. This difference, named Dif-R1R3, allowed evaluating a relative variation for each parameter. The level of significance was fixed at $p<0.05$. Results are presented as mean values ± standard deviation of the mean (SEM).

Results

Average values of all growth plate parameters (three regions combined) are presented for tested and adjacent segments for both control and experimental groups in Table 1. There is a general reduction of all parameters of the tested segments in the experimental group compared to controls, except for those of the number of chondrocytes per column (CC) and proliferative zone height (PZH). At the adjacent segments reductions of less than 8.5% were found for the average growth (AGR) rate and proliferative zone height.

Figure 4 presents results for the Dif-R1R3 of average growth rate in the tested segments. There were significant increases of 121%, 422%, and 117% for Dif-R1R3 when

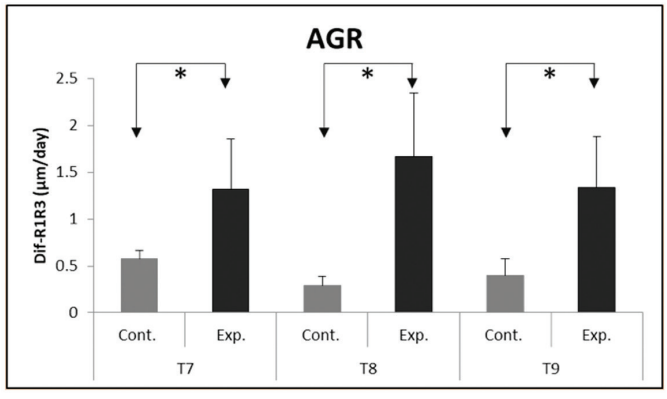

Figure 4. Difference in average growth rates (AGR, µm/day) between regions 1 and 3 (Dif-R1R3) for both experimental (Exp.) and control (Cont.) vertebrae of the tested segments (levels T7, T8 and T9). The difference Dif-R1R3 was significantly higher for the three levels, when comparing the experimental group with the control group (*p<0.05).

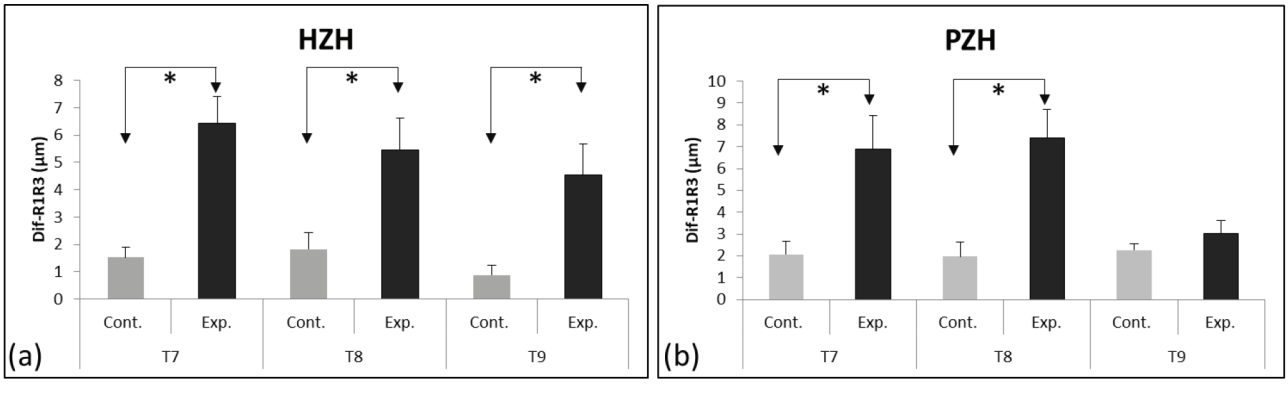

Figure 5. (a) Hypertrophic (HZH) and (b) proliferative (PZH) zones height (µm) in the tested segments. A significantly higher Dif-R1R3 was found for all tested levels (T7, T8, T9) for the HZH when comparing the experimental group (Exp.) with the control one (Cont.). This Dif-R1R3 was also significantly higher at levels T7 and T8 for PZH (*p<0.05).

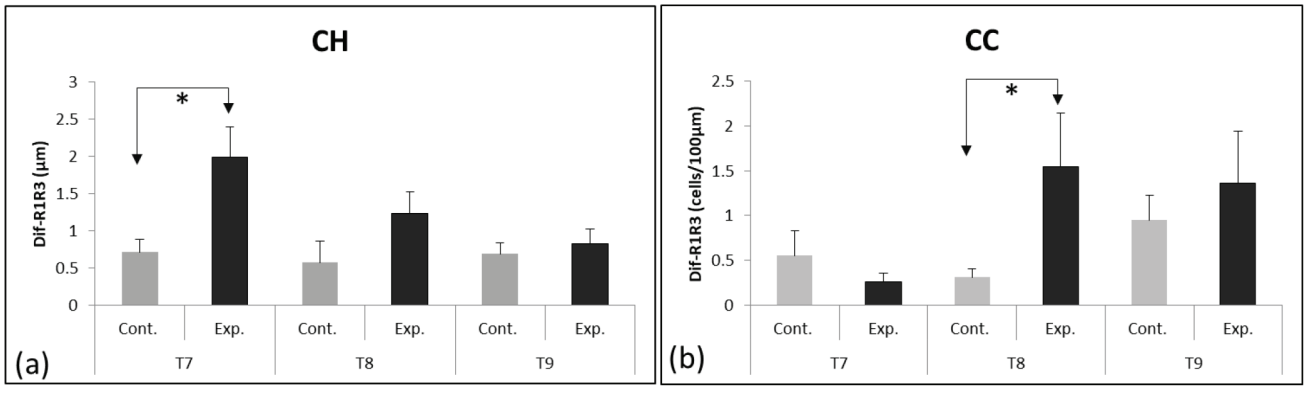

Figure 6. (a) Hypertrophic cells height (CH, µm) and (b) number of proliferative chondrocytes per column (CC, cells/100 µm) in the tested segments. A significantly increased Dif-R1R3 was found for CH at T7 level, and for CC at T8 level (*p<0.05).

comparing the experimental group to the control one, for T7, T8 and T9 levels, respectively. No difference was found between the experimental and control groups when comparing Dif-R1R3 for the adjacent segments (T11-T12, data not shown). The results for the Dif-R1R3 presented in Figure 4 were normalized for the experimental vertebrae to region 1 for T7, T8 and T9 levels (AGR of 8.9 µm/day, 9.3 µm/day and 9.4 µm/day, respectively for this region). Thus, reductions of 15%, 16% and 12%, respectively, were found for the average growth rate within these vertebrae between these two regions. Figure 5 shows results of Dif-R1R3 for hypertrophic and proliferative zone heights of the tested segments. Dif-R1R3 was significantly greater in the experimental group compared to the controls for the hypertrophic zone height (HZH), where increases of 321%, 200%, and 413% were observed for vertebrae T7, T8 and T9, respectively (Figure 5a). Additionally, this difference was also significantly higher at T7 and T8 levels (Dif-R1R3 was increased of 276% and 274%, respectively) for the proliferative zone height when comparing experimental and control groups (Figure 5b).

Results for Dif-R1R3 of hypertrophic cells height (CH) and the number of chondrocytes per column are presented in Figure 6 for the tested segments. For hypertrophic cells height, the Dif-R1R3 was significantly higher for T7 level only, with an increase of 185% in the experimental group compared to controls (Figure 6a). Furthermore, an increase of 394% of Dif-R1R3 was found for the number of chondrocytes per column at T8 when comparing experimental and control groups (Figure 6b). Concerning the adjacent segments (T11-T12), no significant difference was found for Dif-R1R3 for hypertrophic and proliferative zone heights, when comparing experimental and control groups. Similarly, this Dif-R1R3 remains without significant changes for the number of chondrocytes per column and hypertrophic cells height (data not shown).

Discussion

A significant growth modulation after three months of instrumentation was successfully obtained with the new intra-vertebral staple device. This modulation was reflected by a reduced vertebral growth rate from the applied pressure of the implant. This result agrees with studies reported in other animal models undergoing growth plate compression, and follows the well-established Hueter-Volkmann principle. In fact, significant 15 to 30% growth rate reduction have been observed on caudal rat vertebrae under dynamic or static compression[23-25]. Furthermore, our findings showed that this growth modulation was achieved via a significant reduction of the average growth rate near the implant's region (region 3), as observed in other tested vertebral staples. Wakula Y. et al. (2012)[26] found 43% reduction of growth rates in the implant's side between control and experimental animals while evaluating a shape memory alloy intervertebral staple in a pig model. In our study, the achieved reduction within the tested vertebrae between regions 1 and 3 was around 12 to 16%, approximately 3 times less than the reduction reported for devices that span the intervertebral disc[27]. This smaller growth rate reduction within those two regions in the tested vertebrae is likely caused by a non-significant growth rate reduction in the opposite side of the implant observed in this study (of around 11% in region 1) in the experimental group, which is unexpected for this type of devices. We believe that this reduction could be a consequence of the screws length and positioning, since they were long enough to reach this region and, sometimes, deviated from the parallel plane of the growth plate, hence applying pressure over region 1 (Figure 1, T8 level, bottom screw). This event was observed while evaluating the results of average growth rate in 7 from 21 stapled vertebrae (33%) and confirmed by means of postero-anterior and lateral radiographs. Therefore, the potential of the implant could be improved with a better positioning of the screws, or shortened screws while ensuring a sufficient bone fixation.

The effective growth rate modification of a given vertebra, useful for the correction of scoliotic deformities, is in fact the relative combination of the growth rate modulation of the instrumented vs. non instrumented sides generating important changes in the hypertrophic and proliferative zone histomorphometric parameters. Indeed, significant reductions were found in heights of the hypertrophic cells as well as in the proliferative and hypertrophic zones, and in the number of chondrocytes per column when comparing left and right sides of growth plates between experimental and control groups. These histomorphometric changes are not a phenomenon unheard of in animal models following compression. Ménard A-L. et al. (2014)[24] reported, for caudal rat vertebrae dynamically loaded under compression, a significant 17% reduction on the overall growth plate height, 14% decrease in hypertrophic cells height, and 13% decrease in the number of chondrocytes per column between the experimental and control group. These findings are also consistent with those from Valteau B. et al. (2011)[23] in similar experimental conditions, where they found significant reductions of 14% in both hypertrophic and proliferative zone heights, 19% reduction in the number of proliferative cells per column and 15% in hypertrophic cells height. Furthermore, the changes in hypertrophic zone histomorphometric parameters have also been reported for other vertebral staples in a pig model[15]. When evaluating the local effects of a previous one-sided version of the present device, Driscoll M. et al. (2016)[14] found a significant reduction in the hypertrophic zone height of the instrumented vertebrae in contrast with the non-instrumented as well as a reduction on the hypertrophic cells height for instrumented vertebrae compared to the non-instrumented ones. However, these studies did not evaluate the effects of the compression over the proliferative zone. These histomorphometric changes could be associated with the stiffness of the hypertrophic and proliferative zones. Since these zones have been evaluated

as the least rigid growth plate zones, especially in pigs (half as stiff as the reserve zone), they experience the greatest deformation under compression[8,28,29].

The new intra-vertebral staple mainly generated local effects in the epiphyseal growth plates. Indeed, no significant changes on growth rate measurements and histomorphometric parameters were found between control and experimental growth plates of the adjacent levels (T11 and T12). Therefore, we confirm that no curvature was detected at these levels as a compensation mechanism of the pig to maintain the forward looking gaze as reported during the vertebral wedging analysis of this device[21].

In spite of the limitations of this study using a porcine model to test a new device intended for humans and carrying vertebral anatomy differences between the two species, the use of young pigs allowed the local and detailed evaluation of the action of the present device. These results could be extrapolated to humans' spine considering that quadrupeds' spines are mainly axially loaded, due to the action of muscles and ligaments, as in the case of bipeds. During this study, the histological analysis of growth plates was performed considering relative values, such as the difference between regions 1 and 3, rather than comparing absolute values. This approach was chosen to normalize the parameter changes and take into account the possible inter-animal variability in the mechanobiological responses. Results of the present study show only significant alterations of chondrocytes in the proliferative zone in one of the three analyzed vertebrae. The 2D technique used in this study does not allow the visualization of the 3D nature of the proliferative cells columns, preventing the correct visualization of all cells composing a single column. Improvements could be done on this matter by implementing three dimensional stereological methods. In addition, further analyses are needed to confirm the regional effects of the device such as the intervertebral disc health and other connective tissues preservation.

In conclusion, the new two-sided intra-vertebral staple implant achieved a significant growth modulation after three months of instrumentation, associated with a significant reduction in the average growth rate within the instrumented region. At the histomorphometric level, this study showed that both hypertrophic and proliferative zone parameters are major contributors to the average growth rate reduction induced by the implant, with the proliferative and hypertrophic zones being the most mechanically sensitive zones of growth plates. Moreover, the local potential of the implant was also highlighted since no mechanobiological effects were found in the adjacent segments.

References

1. Lonstein J, Carlson J. The prediction of curve progression in untreated idiopathic scoliosis during growth. J bone Jt Surg 1984;66-A(7):1061-1071.
2. Weinstein SL, Dolan LA, Cheng JCY, Danielsson A, Morcuende JA. Adolescent idiopathic scoliosis. Lancet 2008;371(9623):1527-1537.
3. Nault ML, Mac-Thiong JM, Beaudry M, et al. Three-Dimensional spinal morphology can differentiate between progressive and nonprogressive patients with adolescent idiopathic scoliosis at the initial presentation. Spine (Phila Pa 1976) 2014;39(10):601-606.
4. Asher M, Burton D. Adolescent idiopathic scoliosis: natural history and long term treatment effects. Scoliosis J 2006;1(2):1-10.
5. Kiely PJ, Grevitt MP. Recent developments in scoliosis surgery. Curr Orthop 2008;22(1):42-47.
6. Danielsson AJ, Wiklund I, Pehrsson K, Nachemson AL. Health-related quality of life in patients with adolescent idiopathic scoliosis : a matched follow-up at least 20 years after treatment with brace or surgery. Eur Spine J 2001;10(4):278-288.
7. Mehlman C, Araghi A, Roy D. Hyphenated history: the Hueter-Volkmann law. Am J Orthop 1997;26(11):798-800.
8. Villemure I, Stokes IAF. Growth plate mechanics and mechanobiology. A survey of present understanding. J Biomech 2009;42(12):1793-1803.
9. Crawford CH, Lenke LG. Growth modulation by means of anterior tethering resulting in progressive correction of juvenile idiopathic scoliosis: A case report. J Bone Jt Surg 2010;92(1):202-209.
10. Betz RR, Ranade A, Samdani AF, et al. Vertebral Body Stapling. A Fusionless Treatment Option for a Growing Child With Moderate Idiopathic Scoliosis. Spine (Phila Pa 1976) 2010;35(2):169-176.
11. Cobetto N, Aubin CE, Parent S. Surgical planning and follow-up of anterior vertebral body tethering in pediatric idiopathic scoliosis using a patient-specific finite element model integrating growth modulation. (In Press Spine Deform, 2017).
12. Cobetto N, Parent S, Aubin CE. 3D correction over 2 years with anterior vertebral body growth modulation: a finite element analysis of screw positioning, cable tensioning and postoperative functional activities. Clin Biomech 2018;51(2018):26-33.
13. Sarwark J, Aubin CE. Growth Considerations of the Immature Spine. J Bone Jt Surgery-American 2007;89(Suppl 1):8-13.
14. Driscoll M, Aubin CE, Moreau A, Wakula Y, Amini S, Parent S. Novel Hemi-Staple for the Fusionless Correction of Pediatric Scoliosis. Influence on Intervertebral Disks and Growth Plates in a Porcine Model. Clin Spine Surg 2016;29(9):457-464.
15. Bylski-Austrow DI, Wall EJ, Glos DL, Ballard ET, Montgomery A, Alvin H. Spinal Hemiepiphysiodesis Decreases the Size of Vertebral Growth Plate Hypertrophic Zone and Cells. J Bone Jt Surg 2009;91(3):584-593.
16. Carreau JH, Farnsworth CL, Bastrom T, Bryan N, Newton PO. The modulation of spinal growth with nitinol intervertebral stapling in an established swine model. J Child Orthop 2012;6(3):241-253.
17. Hunt KJ, Braun JT, Christensen BA. The Effect of Two Clinically Relevant Fusionless Scoliosis Implant

Strategies on the Health of the Intervertebral Disc. Analysis in an Immature Goat Model. Spine (Phila Pa 1976) 2010;35(4):371-377.
18. Aubin CE, Sarwark JF, Schmid E, Parent S. Fusionless vertebral physeal device and method. US 9,393,058 2016.
19. Schmid E, Aubin CE, Moreau A, Sarwark J, Parent S. A novel fusionless vertebral physeal device inducing spinal growth modulation for the correction of spinal deformities. Eur Spine J 2008;17(10):1329-1335.
20. Driscoll M, Aubin CE, Moreau A, Wakula Y, Sarwark J, Parent S. Spinal growth modulation using a novel intravertebral epiphyseal device in an immature porcine model. Eur Spine J 2012;21(1):138-144.
21. Hachem B, Aubin CE, Parent S. Local Epiphyseal Growth Modulation for the Early Treatment of Progressive Scoliosis: Experimental Validation Using A Porcine Model. Spine (Phila Pa 1976) 2016;41(17):E1009-E1015.
22. Sergerie K, Paren S, Beauchemin P-F, Londoño I, Moldovan F, Villemure I. Growth Plate Explants Respond Differently to *In Vitro* Static and Dynamic Loadings. J Orthop Res 2011;29(4):473-480.
23. Valteau B, Grimard G, Londono I, Moldovan F, Villemure I. *In vivo* dynamic bone growth modulation is less detrimental but as effective as static growth modulation. Bone 2011;49(5):996-1004.
24. Ménard A-L, Grimard G, Valteau B, Londono I, Moldovan F, Villemure I. *In Vivo* Dynamic Loading Reduces Bone Growth Without Histomorphometric Changes of the Growth Plate. J Orthop Res 2014;32(9):1129-1136.
25. Cancel M, Grimard G, Thuillard-Crisinel D, Moldovan F, Villemure I. Effects of *in vivo* static compressive loading on aggrecan and type II and X collagens in the rat growth plate extracellular matrix. Bone 2009;44(2):306-315.
26. Wakula Y, Paren S, Villemure I. Characterization of *in vivo* vertebral growth modulation by shape memory alloy staples on a porcine model for the correction of scoliosis. In: Aubin CE, Stokes I, Labelle H, Moreau A, eds. Research into Spinal Deformities 7. Montreal: IOS Press; 2010:224-225.
27. Song D, Meng C, Zheng G, et al. Effect of staple on growth rate of vertebral growth plates in goat scoliosis. Zhongguo Xiu Fu Chong Jian Wai Ke Za Zhi. 2009;23(1):72-75.
28. Amini S, Veilleux D, Villemure I. Tissue and cellular morphological changes in growth plate explants under compression. J Biomech 2010;43(13):2582-2588.
29. Sergerie K, Lacoursière MO, Lévesque M, Villemure I. Mechanical properties of the porcine growth plate and its three zones fromunconfined compression tests. J Biomech 2009;42(4):510-516.
30. Hachem B. Porcine spine finite element model of progressive experimental scoliosis and assessment of a new dual-epiphyseal growth modulating implant. 2016.